

RESEARCH ARTICLE

Design, synthesis, and biological evaluation of *Helicobacter pylori* inosine 5'-monophosphate dehydrogenase (*Hp*IMPDH) inhibitors

Niteshkumar U. Sahu¹ | Gayathri Purushothaman² | Vijay Thiruvengatam^{2,3} |Prashant S. Kharkar¹ 

¹Department of Pharmaceutical Chemistry, Shobhaben Pratapbhai Patel School of Pharmacy and Technology Management, SVKM's NMIMS, Mumbai, India

²Biological Engineering, Indian Institute of Technology Gandhinagar, Gujarat, India

³Physics, Indian Institute of Technology Gandhinagar, Gujarat, India

Correspondence

Prashant S. Kharkar, Department of Pharmaceutical Chemistry, Shobhaben Pratapbhai Patel School of Pharmacy and Technology Management, SVKM's NMIMS, V. L. Mehta Road, Vile Parle (West), Mumbai, India.

Email: prashant.kharkar@nmims.edu

Inosine 5'-monophosphate dehydrogenase (IMPDH) catalyzes a crucial step in the biosynthesis of guanine nucleotides. Being a validated target for immunosuppressive, antiviral, and anticancer drug development, lately it has been exploited as a promising target for antimicrobial therapy. Extending our previous work on *Mycobacterium tuberculosis* IMPDH, GuaB2, inhibitor development, we screened a set of 23 new chemical entities (NCEs) with substituted flavone (Series 1) and 1,2,3-triazole (Series 2) core structures for their in vitro *Helicobacter pylori* IMPDH (*Hp*IMPDH) and human IMPDH2 (*h*IMPDH2) inhibitory activities. All the NCEs possessed acceptable molecular, physicochemical, and toxicity property profiles. The ranges for *Hp*IMPDH and *h*IMPDH2 inhibition were 9–99.9% and 16–57%, respectively, at 10 μ M concentration. The most potent *Hp*IMPDH inhibitor, **25c**, exhibited IC₅₀ value of 1.27 μ M with no *h*IMPDH2 inhibitory activity. The moderately potent, structurally novel hit molecule, **25c**, may serve as a lead for further design and development of highly potent *Hp*IMPDH inhibitors.

KEYWORDS

1,2,3-triazole, flavone, *Helicobacter pylori*, *h*IMPDH2, *Hp*IMPDH, IMPDH

1 | INTRODUCTION

Helicobacter pylori (*H. pylori*) is a Gram-negative, spiral-shaped bacterial pathogen associated with human gastric mucosa, directly or indirectly causing gastritis, peptic and duodenal ulcers, and gastric adenocarcinoma (Thung et al., 2016; Wroblewski, Peek, & Wilson, 2010). Half of the world's population is infected with *H. pylori*. The dreadful pathogen can survive in the highly acidic environment of the stomach, which is next to impossible for other bacteria. World Health Organization's (WHO) International Agency for Research on Cancer declared *H. pylori* as a Class I gastric carcinogen long back in 1994 (Moss, 2017). Survival in the host acidic environment complicates the treatment of *H. pylori* infection. Many antibiotics are unable to reach therapeutic concentrations in the gastric mucosa due to their acid-labile nature, which leads to decreased efficacy of the standard eradication therapies for *H. pylori* (Zagari, Rabitti, Eusebi, & Bazzoli, 2018). Several alternative treatments have been used to treat these infections (Vakil & Vaira, 2013). In clinical practice, *H. pylori* eradication is

an important challenge due to the increasing prevalence of the multidrug-resistant forms of the deadly pathogen. Several approaches have been tried to develop newer broad-spectrum antibiotics to overcome the resistance (Ezmin, Azlina, & Azilah, 2017; Fuccio et al., 2008; Sahu & Kharkar, 2016; Siddique, Ovalle, Siddique, & Moss, 2018; Tharmalingam, Port, Castillo, & Mylonakis, 2018; Vakil & Vaira, 2013).

In microbial infections, rapid proliferation is an important characteristic, which requires guanine nucleotide pool for the rapidly dividing cells (Shah & Kharkar, 2015). Inosine 5'-monophosphate dehydrogenase (IMPDH) catalyzes the rate-limiting step in the *de novo* biosynthesis of guanine nucleotides, catalyzing the oxidation of inosine 5'-monophosphate (IMP) to xanthosine 5'-monophosphate, which is further converted into guanosine 5'-monophosphate (GMP) by GMP synthase (Figure 1) (Hedstrom, 2009). *H. pylori* would acquire resistance to IMPDH inhibitors if its salvage pathways can provide sufficient guanine nucleotides to support proliferation (Gollapalli et al., 2010), but still *H. pylori* IMPDH (*Hp*IMPDH) inhibitors have the

antibiotic potential due to the large requirement of guanine nucleotides for cell proliferation (Hedstrom, Liechti, Goldberg, & Gollapalli, 2011).

Recently, IMPDH inhibitors have been explored as potential antimicrobial agents. These investigations have resulted in the development of several potent and selective agents (Petrelli et al., 2013). In an interesting study, *Cryptosporidium parvum* IMPDH (CpIMPDH) inhibitors were screened against several bacterial pathogens, generating lead molecules that could be further optimized (Shah & Kharkar, 2015). All reported CpIMPDH inhibitors have common pharmacophoric features—two aromatic rings separated by a linker (Figure 2) (Sahu, Singh, Ferraris, Rizzi, & Kharkar, 2018). Screening of these molecules against *Hpl*IMPDH led to the identification of **C91** (9, Figure 2), the most potent *Hpl*IMPDH inhibitor, belonging to 1*H*-benzimidazole series with $IC_{50} = 8$ and 1.1 nM for CpIMPDH and *Hpl*IMPDH, respectively (Gollapalli et al., 2010; Hedstrom et al., 2011). The 1*H*-benzimidazoles, phthalazinones, quinoline-2-ones, and related chemotypes (Figure 2) may not make a good drug candidate due to several issues including, but not limited to, poor metabolic stability, in addition to others (Hedstrom et al., 2011). Given the relative lack of interesting chemotypes for *Hpl*IMPDH inhibitor development, we started off with the objective of finding newer, potent *Hpl*IMPDH inhibitors possessing acceptable molecular, physicochemical, pharmacokinetic, and toxicity property profiles.

Our previous work on *Mycobacterium tuberculosis* (*Mtb*) IMPDH, GuaB2, inhibitor development (Sahu et al., 2018) was the main motivation for us to venture into this new territory where only few groups are working across the globe. Interestingly, the sequence identity between *Mtb*GuaB2 and *Hpl*IMPDH was observed to be 55.77% (Table S1, Supporting Information). It was perfectly logical, given the higher sequence identity between the two enzymes, to explore the modestly potent *Mtb*GuaB2 inhibitors identified previously by us for potential *Hpl*IMPDH inhibitory activity. In addition to our 1,2,3-triazole *Mtb*GuaB2 inhibitors (Sahu et al., 2018), we designed few molecules containing the requisite pharmacophoric features discussed above, belonging to flavone class.

Flavones, one of the most well-known privileged substructures in drugs and drug-like structures, are an important class of heterocycles, mainly found in fruits, vegetables, coffee, tea, etc. (Singh, Kaur, & Silakari, 2014). These molecules belong to a broader class of flavonoids possessing 2-phenylchromen-4-one (2-phenyl-1-benzo[*b*]pyran-4-one) as a core structure. Few naturally occurring flavones such as apigenin, luteolin, and wogonin contain 2-substituted aryl flavone substructure. Their derivatives have been reported to exhibit a wide range of biological effects. Furthermore, 2-substituted aryl flavones

have been attractive lead structures owing to their broad spectrum of pharmacological activities, mainly anti-inflammatory (Serafini, Peluso, & Raguzzini, 2010), anticancer (Gallus, Juvale, & Wiese, 2014), antioxidant (Venkatachalam, Nayak, & Jayashree, 2012), and antimicrobial (Cushnie & Lamb, 2005; Fericola et al., 2015; Isobe, Doe, Morimoto, Nagata, & Ohsaki, 2006). Similarly, 1,2,3-triazole moiety is yet another much sought-after privileged substructure (N-heterocycles family). It occurs as a key building block in several pharmaceutical agents. With reference to microbial IMPDH inhibitors, CpIMPDH (Maurya et al., 2009) and *Mtb*GuaB2 (Sahu et al., 2018) inhibitors have been reported to contain 1,2,3-triazole core structure. Our previous in vitro screening campaign against *Mtb*GuaB2 led to the identification of 1,2,3-triazole containing hits (**24a**, **24b**, and **26a**, Table 2) (Sahu et al., 2018) active in *Mtb* whole-cell ($MIC_{90} = 50 \mu\text{M}$) and biochemical assays for *Mtb*GuaB2 inhibition (**24a**, 35% and **26a**, 52.24% inhibition, at 50 μM) (Sahu et al., 2018). In this study, by learning from our previous stint with microbial IMPDH inhibitor development, we report the design, synthesis, and biological evaluation of *Hpl*IMPDH inhibitors belonging to flavone (Series 1) and 1,2,3-triazole (Series 2) chemotypes. The design process was based on the essential features required for microbial IMPDH inhibitors—two aromatic rings separated by a suitable linker. To rationalize the design process, comparative protein (or homology) model of *Hpl*IMPDH was developed and used for the structure-based design of potential inhibitors. The details of the homology modeling procedure and docking studies can be found elsewhere (Supporting Information). In case of flavone series, the chromone nucleus served as one of the aromatic rings, whereas in the other series, 1,2,3-triazole served as part of the linker, based on a similar linker in the most potent *Hpl*IMPDH inhibitor **C91** (9, Figure 2). The hits identified in this investigation are likely to motivate interested researchers to further explore these chemotypes for the design and development of highly potent and structurally novel *Hpl*IMPDH inhibitors, a hard nut to crack.

2 | EXPERIMENTAL SECTION

2.1 | Chemistry

2.1.1 | General procedure for synthesis of chalcone derivatives (12a-h) (Juvale, Stefan, & Wiese, 2013)

An aqueous solution of NaOH (20%, 5 mL) was added dropwise to a previously cooled mixture of 2'-hydroxyacetophenone **11** (5 mmol) and substituted carboxaldehyde **10a-h** (5 mmol) in absolute EtOH (25 mL) under vigorous stirring. The mixture was stirred at room temperature (RT) for 24–72 hrs. After reaction completion

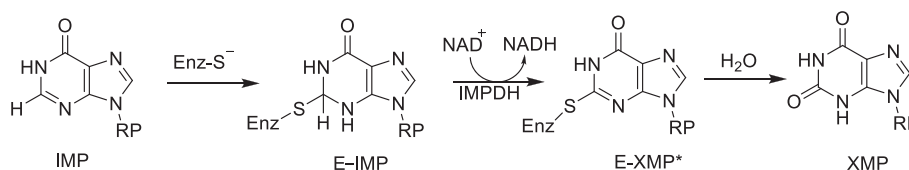


FIGURE 1 Steps involved in the catalytic cycle of IMPDH (conversion of inosine 5'-monophosphate [IMP] to xanthosine 5'-monophosphate [XMP]) during de novo biosynthesis of guanine nucleotides. aRP, ribofuranosyl-5'-monophosphate; Enz, enzyme; E-IMP, IMP/IMPDH adduct; E-XMP*, IMPDH/XMP thioimidate intermediate

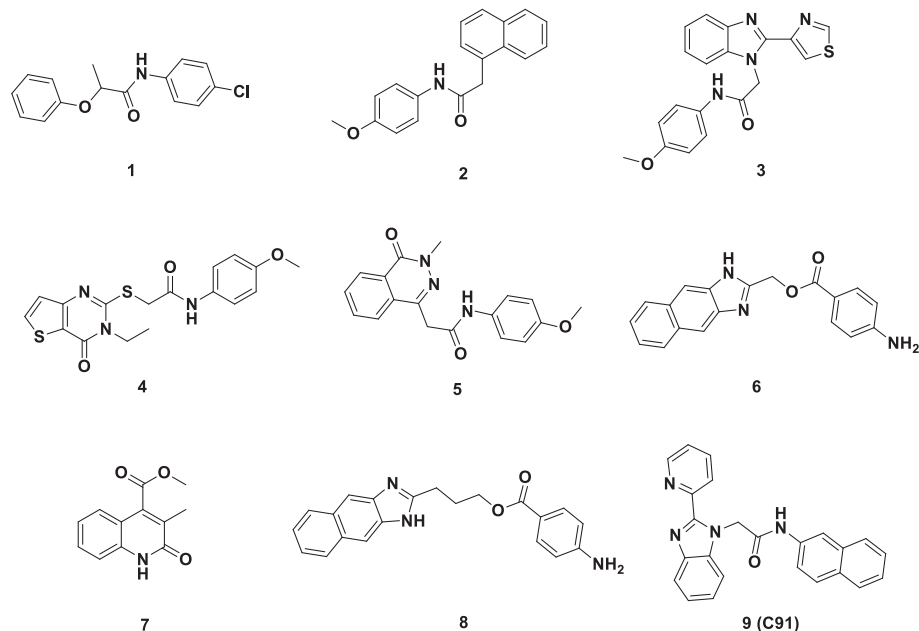


FIGURE 2 *Helicobacter pylori* IMPDH (*HpIMPDH*) inhibitors reported in the literature so far

(as indicated by thin layer chromatography (TLC)), the mixture was poured onto crushed ice and acidified with dilute HCl. The precipitated solid was filtered at suction and washed with water. The crude product was recrystallized from absolute EtOH to get crystalline, substituted chalcone (**12a-h**).

2.1.2 | General procedure for synthesis of 3-hydroxy-2-substituted flavones (**13a-h**) (Juvale et al., 2013)

Appropriate chalcone (**12a-h**) (5 mmol) was dissolved in absolute EtOH (25 mL). Aqueous NaOH (25%, 10 mL) and H₂O₂ (25%, 10 mL) were added slowly and stirred overnight at RT. Reaction was monitored by TLC. After completion, the reaction mixture was quenched with crushed ice and acidified with dilute HCl. The precipitate was filtered in vacuo, washed with water, and dried. Recrystallization of the crude product was recrystallized from absolute EtOH yielded pure **13a-h**.

2.1.3 | General procedure for synthesis of substituted acetamides (**15a-c**) (Sahu et al., 2018)

To a mixture of substituted aniline (**14a-c**) (20.1 mmol) and TEA (24.12 mmol, 1.2 equiv.) in dry THF, chloroacetyl chloride (22.11 mmol, 1.1 equiv.) was added dropwise with the help of pressure-equalizing tube, at 0 °C. After completion, the triethylammonium salt was filtered off and the reaction mixture was concentrated in vacuo, followed by washing and air-drying, to obtain crude substituted acetamide derivatives (**15a-c**).

2.1.4 | General procedure for synthesis of *N*-(1-oxo-1,3-dihydroisobenzofuran-5-yl)acetamide derivatives (**16a-n**) (Sahu et al., 2018)

A reaction mixture containing **13a-h** (0.44 mmol) and K₂CO₃ (0.18 g, 1.33 mmol) in dry DMF (3 mL) was stirred for 16 hrs. After completion, the reaction mixture was quenched with brine (2 × 50 mL). The precipitated solid was filtered off, washed with water, and dried under

vacuo. The crude product was further purified by column chromatography using CHCl₃:MeOH (9:1) as mobile phase.

2.1.5 | General procedure for synthesis of substituted 1,2,3-triazole derivatives (**24/25/26a-c**) (Sahu et al., 2018)

Synthesis of substituted 1,2,3-triazole derivatives **24/25/26a-c** was carried out according to the previously reported work on *MtbGuaB2* inhibitor development. (Sahu et al., 2018).

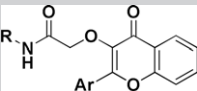
2.2 | Biological evaluation

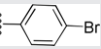
2.2.1 | In vitro *HpIMPDH* inhibition assay

A total of 26 molecules were screened in vitro at 10 μM concentration. The assay was performed in a 200 μL final volume in Black 96-Well Plate (Tarsons Products Pvt. Ltd., Kolkata, India) with a reaction buffer composed of 50 mM Tris-HCl (pH 8.6), 100 mM KCl, and 1 mM dithiothreitol (DTT). Assays were performed using 100 nM *HpIMPDH* in the presence or absence of test compounds. The assay mixture was incubated for 10 min at 37 °C, and reaction was initiated by the addition of 250 μM of IMP and 300 μM of NAD⁺ (substrate buffer). The assay was allowed to proceed at 37 °C for 45 min. Generated NADH was measured by reading the fluorescence (excitation 340 nm, emission 440 nm) at an interval of 1 min using PerkinElmer EnVision Multilabel Reader (Waltham, MA). Compound **9 (C91)** (1 μM) was used as a positive control and DMSO as a vehicle control. For IC₅₀ determination, a total of 10 concentrations ranging from 50 nM to 25 μM, in triplicates were used. Enzyme inhibition and IC₅₀ values were expressed in % inhibition and μM, respectively.

2.2.2 | In vitro *hIMPDH2* inhibition assay

The *hIMPDH2* was purchased from NovoCIB SAS (Lyon, France) and used for in vitro screening of 26 molecules at 10 μM concentration. The assay was performed in 96-well plates (Tarsons, 980040) (200 μL final volume) with a reaction buffer composed of 100 mM Tris-HCl

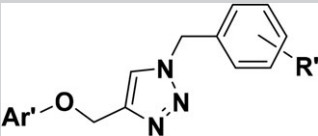
TABLE 1 Biological activity data of the new chemical entities belonging to substituted flavones (Series 1)


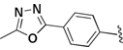
Compound code	R	Ar	<i>Hpl</i> IMPDH ^a		<i>h</i> IMPDH2% Inhibition (10 μ M) ^a
			% Inhibition (10 μ M)	IC ₅₀ (μ M)	
C91 ^b					0.197 \pm 0.08
16a		4-CH ₃ Ph	16.57 \pm 1.3	ND	0.10
16b		4-OCH ₃ Ph	9.13 \pm 1.2		0.10
16c		4-CH ₃ Ph	10.24 \pm 2.3		0.10
16d		4-OCH ₃ Ph	15.31 \pm 1.1		2.10 \pm 0.09
16e		3,4-diOCH ₃ Ph	53.81 \pm 2.95		0.10
16f		3,4,5-triOCH ₃ Ph	27.42 \pm 1.8		16.54 \pm 0.12
16g		Ph	53.81 \pm 2.95		0.10
16h		4-CH ₃ Ph	16.62 \pm 3.5		0.10
16i		4-OCH ₃ Ph	99.89 \pm 2.12	1.88 \pm 0.07	56.81 \pm 0.95
16j		3,4-diOCH ₃ Ph	57.98 \pm 2.75	ND	34.45 \pm 1
16k		3,4,5-triOCH ₃ Ph	58.99 \pm 4.86		0.10
16l		2-ClPh	12.14 \pm 2.15		0.10
16m		Furan-2-yl	52.46 \pm 3.5		0.10
16n		Thien-2-yl	53.31 \pm 1.6		0.10

Note. ND = not determined.

^a All data are expressed as \pm SD (average of $n = 3$). IC₅₀ values were determined for compounds with % inhibition \sim 70% or more at 10 μ M concentration.

^b Yet unpublished data (manuscript under review).

TABLE 2 Biological activity data of the new chemical entities belonging to substituted 1,2,3-triazoles (Series 2)


Compound code	Ar'	R'	<i>Hpl</i> IMPDH ^a		<i>Mtb</i> GuaB2% Inhibition (50 μ M) ^b	<i>h</i> IMPDH2% Inhibition (10 μ M) ^a
			% Inhibition (10 μ M)	IC ₅₀ (μ M)		
24a		3-OCH ₃	99.89 \pm 2.3	4.06 \pm 0.11	71.0 \pm 0.6	0.10
24b		3-cl	58.44 \pm 2.05	ND	72.6 \pm 8.4	0.10
24c		3,4-Cl ₂	55.14 \pm 3.95		ND	0.10
25a		3-OCH ₃	23.86 \pm 1.32		ND	30.66 \pm 0.65
25b		3-cl	69 \pm 1.9	2.1 \pm 0.1	ND	0.10
25c		3,4-Cl ₂	69.66 \pm 2.96	1.27 \pm 0.08	ND	0.10
26a		3-OCH ₃	31.48 \pm 1.45	ND	52.4 \pm 8.0	24.94 \pm 0.32
26b		3-cl	37.8 \pm 2.66		ND	0.10
26c		3,4-Cl ₂	34.58 \pm 3.36		ND	0.10

Note. ND = not determined.

^a All the data are expressed as \pm SD (average of $n = 3$).

^b Values taken from "Hit discovery of *Mycobacterium tuberculosis* inosine 5'-monophosphate dehydrogenase, GuaB2, inhibitors," by N. U. Sahu et al., 2018, *Bioorganic & Medicinal Chemistry Letters*, 28(10), pp. 1714–1718; IC₅₀ values were determined for compounds with % inhibition \sim 70% or more at 10 μ M concentration.

(pH 8.6), 100 mM KCl, and 5 mM DTT, 4% vol/vol DMSO plus or minus test compound and 0.15 mU of purified *h*IMPDPH2 enzyme per well (from 1.5 mg/mL stock concentration). The final volume of the enzyme stock solution per well was 2 μ L, which was insignificant to cause any change in the final assay buffer composition. The reaction was initiated by the addition of (substrate buffer) 0.2 mM of IMP and 0.2 mM of NAD⁺, and the assay was allowed to proceed at 37 °C for 30 min. The generated NADH was measured by reading the absorbance at 340 nm. At this wavelength, a background of <0.1 optical density was observed with negligible cross talk between wells. Mycophenolic acid (10 μ M) was used as a positive control and DMSO as a vehicle control. Enzyme inhibition at 10 μ M concentration was expressed in percentage (Dunkern et al., 2012, 2014; Shah & Kharakar, 2018).

2.2.3 | Data analysis

The inhibition of *Hpl*IMPDPH and *h*IMPDPH2 by the new chemical entities (NCEs) was investigated by monitoring the change in the initial velocity of NADH formation (fluorescence and absorbance). To calculate the IC₅₀ values, initial velocity of the reaction was calculated for the period of 10 min after initiation of the reaction and was plotted against concentrations of the NCEs. The IC₅₀ values were calculated for each compound by fitting the data in Equation (1) with the help of GraphPad Prism version 6.0 (La Jolla, CA, <http://www.graphpad.com>).

$$Y = \text{Bottom} + (\text{Top} - \text{Bottom}) / (1 + 10^{([\text{LogIC}_{50} - X]) * \text{HillSlope}}) \quad (1)$$

2.3 | Computational studies

2.3.1 | Hardware and software

All the molecular modeling studies were performed on HP laptop (Intel® Core™ i7-5500U CPU @ 2.40 GHz, RAM 4 GB) running Windows 8.1 Home Basic Operating System. Schrödinger Small-Molecule Drug Discovery Suite Release 2016-1 (Schrödinger, LLC, New York, NY2016-1), and the products included therein were used for performing docking studies. In silico preclinical toxicity end points (mutagenicity, genotoxicity, and carcinogenicity) predictions were carried out using CASE Ultra (1.6.2.3) software (MultiCASE Inc., Beachwood, OH; Saiakhov, Chakravarti, & Klopman, 2013; Saiakhov, Chakravarti, & Sedykh, 2014).

2.3.2 | Homology modeling and molecular docking

All the methodical details related to pairwise sequence alignment, homology modeling, and molecular docking studies are provided in Supporting Information. In brief, a homology model of *Hpl*IMPDPH was developed for structure-based design of potential inhibitors. The selected model was then put to use for investigating the binding mode(s) of the designed compounds with *Hpl*IMPDPH.

2.3.3 | In silico toxicity predictions

CASE Ultra is a quantitative structure–activity relationship software for predicting toxicity of the chemicals. The CASE Ultra models cover a wide variety of preclinical toxicity end points and are claimed to be the largest collection of high-quality computational models; several models have been and/or being developed in collaboration with USFDA. Table S4 (Supporting Information) lists the CASE Ultra models

used in this investigation. The results of in silico toxicity predictions for the mutagenicity, genotoxicity, and carcinogenicity end points are given in Table 3. The molecular, physicochemical, and pharmacokinetic property predictions are given in Table S5 (Supporting Information).

3 | RESULTS AND DISCUSSION

3.1 | Chemistry

Substituted chalcones (**12a–h**) were synthesized using modified Claisen–Schmidt condensation reaction between carboxaldehydes (**10a–h**) and 2'-hydroxyacetophenone (**11**), and cyclized in the presence of H₂O₂/NaOH to yield 3-hydroxy-2- substituted aryl flavones (**13a–h**, Scheme 1) (Juvale et al., 2013). Aromatic amines (**14a–c**) were condensed with chloroacetyl chloride in the presence of TEA to give substituted acetamides (**15a–c**). Furthermore, 3-hydroxy-2-substituted aryl flavones (**13a–h**) were subjected to O-alkylation with **15a–c** in the presence of anhydrous K₂CO₃/dry DMF to yield the NCEs (**16a–h**, Table 1). Synthesis of 1,2,3-triazole derivatives was proceeded in two steps as described previously (Schemes 2–4) (Sahu et al., 2018).

3.2 | Biological evaluation

3.2.1 | Enzyme inhibition assays

All the NCEs were tested for in vitro *Hpl*IMPDPH and *h*IMPDPH2 inhibition which was measured by monitoring the production of NADH at NCE concentration of 10 μ M. Molecules exhibiting ~70% or more *Hpl*IMPDPH inhibition were taken further for IC₅₀ determination by using NCE concentration range of 50 nM to 25 μ M. To generate the concentration–response curves, average of fluorescence responses at plateau of fluorescence–time curves of all inhibitors was plotted against their corresponding logarithmic concentrations in case of *Hpl*IMPDPH. The activity data (% inhibition and IC₅₀, wherever applicable) of the NCEs are given in Table 1 (Series 1) and Table 2 (Series 2).

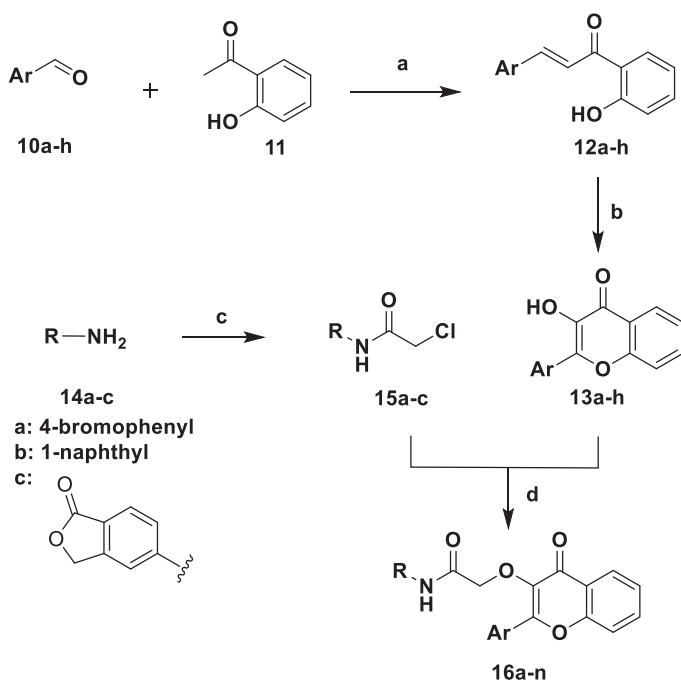
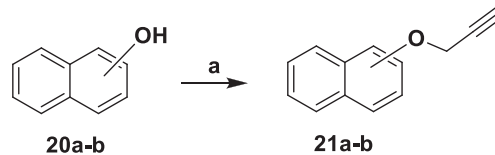
In case of flavone series, the pharmacophoric features—two (hetero)aromatic rings—were explored systematically while keeping the linker, that is, oxyacetamide, constant. Three variants of the (hetero) aromatic ring on the left side (R group, Table 1) were tried. Of these, only 5-substituted phthalide substructure yielded moderately potent inhibitors in the series for similar substituents tried at the second position of the flavone core structure (**16i**, Table 1). The corresponding compounds with other two R groups were inactive (**16b** and **16d**) at *Hpl*IMPDPH. Increasing the number of –OCH₃ substituents on the Ar group on the flavone core increased the potency for the naphthalene variant (Feature A) (**16d** vs. **16e**) while for the phthalide variant, similar structural modification halved the % inhibition (**16i** vs. **16j**). Compound **16i** also inhibited *h*IMPDPH2 significantly (Table 1). The differential % *Hpl*IMPDPH inhibition by three variants (R groups) could be attributed to the presence or absence of a H-bond acceptor functionality such as lactone ring of the phthalide variant. The selectivity for *Hpl*IMPDPH over its human counterpart was evident for the 1-naphthyl variant over the phthalide variant (**16e** vs. **16j**). Also, addition of a hydrophobic 4-CH₃ substituent on the aromatic ring decreased the % inhibition by threefold (**16g** vs. **16h**), indicating the fact that either

TABLE 3 In silico toxicity predictions for the hit molecules

Sr. no.	Model name	C91	16i	25b	25c
Bacterial mutagenicity models (ICH M7)					
1	GT1_A7B	#	#	#	#
2	GT1_AT_ECOLI	#	+	#	#
3	GT_EXPERT	–	–	+	+
4	PHARM_SALM	\$	–	–	–
5	PHARM_ECOLI	–	+	–	–
Genotoxicity models					
6	GT2_A7U	+	+	+	+
7	GT2_A7V	\$	#	#	#
8	GT2_A7W	+	+	+	+
9	GT2_A7X	#	+	+	+
10	GT2_A8H	\$	#	\$	\$
11	GT3_A7S	\$	–	–	–
12	GT3_A7T	#	#	#	+
13	GT3_A8J	+	+	+	+
14	GT4_A7N	+	+	+	+
Carcinogenicity models					
15	AF1	+	–	–	–
16	AF2	+	–	–	–
17	AF3	+	–	–	–
18	AF4	+	+	–	–
19	AFU	+	–	–	–
20	AFV	+	+	–	–
21	AFW	+	–	–	–

Note. + Positive; – Negative; # Inconclusive; \$ Out of domain.

there was enough space to accommodate unsubstituted Ph ring or a hydrophobic substituent was not tolerated on the Ph ring. Replacing the 4-CH₃ substituent with 4-OCH₃ picked up the potency for both the enzymes (**16h** vs. **16i**), emphasizing the need for a polar H-bond

**SCHEME 1** Synthesis of substituted flavones**SCHEME 2** Synthesis of intermediates for 1,2,3-triazole series

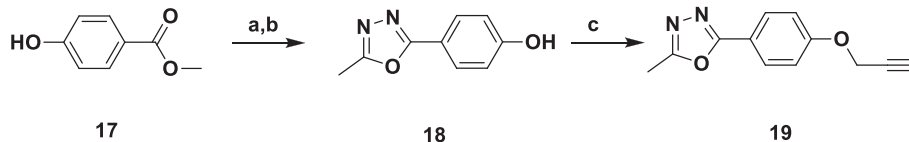
acceptor group at this strategic position. Increasing the number of –OCH₃ substituents on the Ar group (flavone core) in phthalide variant had pronounced effect on % inhibition of hIMPDPH2. With each additional –OCH₃ group, the hIMPDPH2 inhibition drastically reduced (**16i**, **16j** and **16k**). In case of HplIMPDPH, there was twofold reduction in inhibitory potential (**16i** vs. **16j**) and further retention of activity (**16j** to **16k**). Further tinkering (mix-and-match) with the structural features in this series may yield more potent and selective HplIMPDPH inhibitors.

For 1,2,3-triazole series, three different mono- or bicyclic (hetero) aromatic variants were tried on the left side of the linker (Ar') such as 4-(5-methyl-1,3,4-oxadiazol-2-yl)phenyl (**24a-c**), 1-naphthyl (**25a-c**) and 2-naphthyl (**26a-c**) (Table 2) while keeping the substituents on the phenyl ring (R') on the right side of the 1,2,3-triazole nucleus (3-OCH₃, 3-Cl, 3,4-Cl₂) constant. The most potent compound (**24a**, Table 2), with 4-(5-methyl-1,3,4-oxadiazol-2-yl)phenyl variant, exhibited >99% HplIMPDPH inhibition. The corresponding compounds from the other two variants were fourfold (**25a**) and threefold (**26a**) less active than **24a**. Some degree of conformational freedom was expected in this part (Ar') of the NCEs. This may also emphasize narrower binding region for this part of the inhibitor, in addition to the requirement for H-bond acceptor functionality. The substituents on the phenyl ring on the right side (R'), particularly, 3-Cl and 3,4-Cl₂ were equipotent for each of the three variants (**24b** and **24c**, **25b** and **25c**, and **26b** and **26c**). In addition, the other two variants, that is, 1- and 2-naphthyl, with 3-OCH₃ substituents were nearly equipotent for the human and HplIMPDPH enzymes (**25a** vs. **26a**). It was very interesting to observe subtle changes in the structure leading to pronounced changes in the % inhibition and selectivity for HplIMPDPH over hIMPDPH2 (Table 2). The most potent and selective compound (**25c**) belonged to 1-naphthyl variant. Compound **25b** was a close competitor with respect to the potency and selectivity for the HplIMPDPH. Overall, we found an interesting mix-and-match of the structural features in these series of HplIMPDPH inhibitors. The structure–activity relationship (SAR) trends shed light on the precise requirements for potency and selectivity of these molecules for the two enzymes.

3.3 | Computational studies

3.3.1 | Homology modeling and molecular docking

The homology model of HplIMPDPH tetramer was generated using *Streptococcus pyogenes* IMPDPH as the template (PDB ID 1ZFJ, Resolution 1.9 Å) (Zhang et al, 1999) identified by SWISSMODEL. The best model with good stereochemical quality, after thorough protein preparation tasks, was then used for docking studies of the designed molecules. The details of the complete process (pairwise sequence alignment, homology model generation, and molecular docking) can be found in the Supporting Information (Tables S1–S3 and Figures S1–S4). Docking



SCHEME 3 Synthesis of 1- and 2-(prop-2-ynoxy)naphthalenes

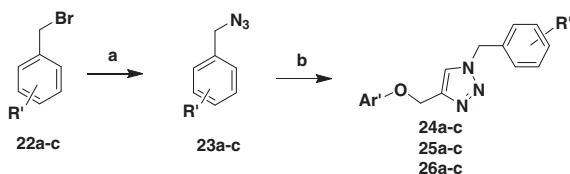
scores of the select few hits were reported (Supporting Information). These scores were in good agreement with the observed experimental values, that is, IC_{50} (Tables 1 and 2, Supporting Information Table S3). The binding mode (Figure 3) could clearly demonstrate crucial interactions between the ligands and the corresponding residues in *Hpl*IMPDH, validating our design strategy. As seen in Figure 3, the hit **25c** nicely occupied the area of the ligand-binding site next to IMP. The purine ring of IMP was involved in face-to-face π - π stacking interaction with the 2,4-dichlorophenyl substituent of **25c**. The bent conformation of the molecule due to the 1,2,3-triazole linker oriented the distal Ph ring such that one of the Cl substituents (4-Cl) interacted with the carbonyl (C=O) of Asn272. In addition, the 1-naphthyl substituent was located in a hydrophobic pocket lined by several hydrophobic residues. Overall, the binding mode clearly revealed potential interactions of the hit **25c** with the residues lining the ligand-binding pocket of *Hpl*IMPDH.

3.3.2 | In silico toxicity prediction profiles of the NCEs

Table 3 lists the outcome of in silico toxicity (mutagenicity, genotoxicity, and carcinogenicity) prediction of the hits **16i**, **25b**, and **25c** along with the standard *Hpl*IMPDH inhibitor, C91. As seen in Table 3, compound **16i** was predicted as positive for mutagenicity. Detailed analysis of the results showed that the lactone substructure in **16i** was flagged, thereby predicting the compound to be mutagenic (data not shown). For carcinogenicity predictions, **C91** was predicted as carcinogenic by all the models, while **16i** was flagged by two models. Other two compounds—**25b** and **25c**—were predicted to be noncarcinogenic. In case of genotoxicity, the predictions were mixed; some were positive, a few were negative, and many were either inconclusive or outside the domain of predictability of the model(s) used. Although these predictions provide guidance, they should be used with caution; ideally such predictions should be combined with medicinal chemist's experience and intuition.

4 | CONCLUSION

This study, based on our experience with microbial IMPDH and *h*IMPDH2, led to fruition with respect to exploring an unknown territory, that is, *Hpl*IMPDH inhibitor discovery. Our efforts focused on



Reagents and conditions. a. NaN_3 , *i*-PrOH:H₂O (4:1); b. **19/21a/21b**, Cu(OAc)₂, *t*-BuOH:H₂O (3:1), RT, 8 h

SCHEME 4 Synthesis of 1,2,3-triazole NCEs

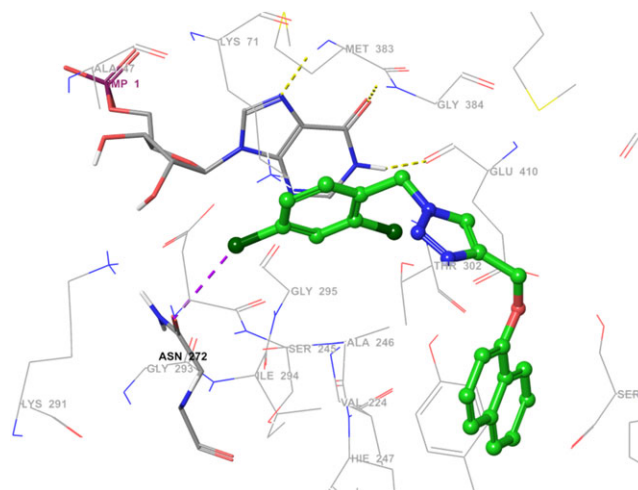


FIGURE 3 Binding mode of **25c** into the ligand-binding site of *Hpl*IMPDH homology model. The ligand is shown as ball-and-stick model, while the enzyme residues are shown as line models colored by the element. Gray dotted lines indicate interaction ligand Cl atom with Asn272 C=O group. π - π stacking interaction of the dichlorophenyl ring from ligand and the purine ring of IMP is clearly visible

systematically exploring the SAR certainly led to moderately potent, selective over the human enzyme and structurally novel *Hpl*IMPDH inhibitors. The criticality of the work lies in the identification of on-and-off structural features desired for the potency and selectivity. The key learnings from this thoughtful study are likely to contribute to development of potent and selective *Hpl*IMPDH inhibitors in near future. This will certainly open up new treatment avenues for the dreadful bacterial infection potentially troubling every other person on the planet.

ACKNOWLEDGMENTS

Niteshkumar U. Sahu received PhD fellowship from SVKM's NMIMS, Mumbai, India. Niteshkumar U. Sahu and Prashant S. Kharkar deeply acknowledge the help received from Sivapriya Kirubakaran, Assistant Professor, Chemistry and Bioengineering, Indian Institute of Technology Gandhinagar, Gujarat, India, Kapil Juvale, Assistant Professor with SVKM's NMIMS, Shobhaben Pratapbhai Patel School of Pharmacy and Technology Management, Mumbai, India, and Chetan Shah, PhD student in PK's group during IMPDH inhibition assays and preparation of the article.

CONFLICTS OF INTEREST

The authors declare no potential conflict of interests.

ORCID

Prashant S. Kharkar  <https://orcid.org/0000-0003-1955-7223>

REFERENCES

- Cushnie, T. P. T., & Lamb, A. J. (2005). Antimicrobial activity of flavonoids. *International Journal of Antimicrobial Agents*, 26(5), 343–356.
- Dunkern, T., Chavan, S., Bankar, D., Patil, A., Kulkarni, P., Kharkar, P. S., ... Makhija, M. T. (2014). Design, synthesis and biological evaluation of novel inosine 5'-monophosphate dehydrogenase (IMPDH) inhibitors. *Journal of Enzyme Inhibition and Medicinal Chemistry*, 29(3), 408–419.
- Dunkern, T., Prabhu, A., Kharkar, P. S., Goebel, H., Rolser, E., Burckhard-Boer, W., ... Makhija, M. T. (2012). Virtual and experimental high-throughput screening (HTS) in search of novel inosine 5'-monophosphate dehydrogenase II (IMPDH II) inhibitors. *Journal of Computer-Aided Molecular Design*, 26(11), 1277–1292.
- Ezmin, A., Azlina, I., & Azilah, S. (2017). Papr reduction using scs-slm technique in stfbc mimo-ofdm. *ARNP Journal of Engineering and Applied Sciences*, 12(10), 3218–3221.
- Fernicola, S., Torquati, I., Paiardini, A., Giardina, G., Rampioni, G., Messina, M., ... Cutruzzolà, F. (2015). Synthesis of triazole-linked analogues of c-di-GMP and their interactions with diguanylate cyclase. *Journal of Medicinal Chemistry*, 58(20), 8269–8284.
- Fuccio, L., Laterza, L., Zagari, R. M., Cennamo, V., Grilli, D., & Bazzoli, F. (2008). Treatment of *Helicobacter pylori* infection. *British Medical Journal*, 337(7672), 746–750.
- Gallus, J., Juvale, K., & Wiese, M. (2014). Characterization of 3-methoxy flavones for their interaction with ABCG2 as suggested by ATPase activity. *Biochimica et Biophysica Acta—Biomembranes*, 1838(11), 2929–2938.
- Gollapalli, D. R., MacPherson, I. S., Liechti, G., Gorla, S. K., Goldberg, J. B., & Hedstrom, L. (2010). Structural determinants of inhibitor selectivity in prokaryotic IMP dehydrogenases. *Chemistry and Biology*, 17(10), 1084–1091.
- Hedstrom, L. (2009). IMP dehydrogenase: Structure, mechanism, and inhibition. *Chemical Reviews*, 109(7), 2903–2928.
- Hedstrom, L., Liechti, G., Goldberg, J. B., & Gollapalli, D. R. (2011). The antibiotic potential of prokaryotic IMP dehydrogenase inhibitors. *Current Medicinal Chemistry*, 18(13), 1909–1918.
- Isoabe, T., Doe, M., Morimoto, Y., Nagata, K., & Ohsaki, A. (2006). The anti-*Helicobacter pylori* flavones in a Brazilian plant, *Hyptis fasciculata*, and the activity of methoxyflavones. *Biological & Pharmaceutical Bulletin*, 29(5), 1039–1041.
- Juvale, K., Stefan, K., & Wiese, M. (2013). Synthesis and biological evaluation of flavones and benzoflavones as inhibitors of BCRP/ABCG2. *European Journal of Medicinal Chemistry*, 67, 115–126.
- Maurya, S. K., Gollapalli, D. R., Kirubakaran, S., Zhang, M., Johnson, C. R., Benjamin, N. N., ... Cuny, G. D. (2009). Triazole inhibitors of *Cryptosporidium parvum* inosine 5'- monophosphate dehydrogenase. *Journal of Medicinal Chemistry*, 52(15), 4623–4630.
- Moss, S. F. (2017). The clinical evidence linking *Helicobacter pylori* to gastric cancer. *Cellular and Molecular Gastroenterology and Hepatology*, 3(2), 183–191.
- Petrelli, R., Vita, P., Torquati, I., Felczak, K., Wilson, D. J., Franchetti, P., & Cappellacci, L. (2013). Novel inhibitors of inosine monophosphate dehydrogenase in patent literature of the last decade. *Recent Patents on Anti-Cancer Drug Discovery*, 8(2), 103–125.
- Sahu, N. U., & Kharkar, P. S. (2016). Computational drug repositioning: A lateral approach to traditional drug discovery? *Current Topics in Medicinal Chemistry*, 16(19), 2069–2077.
- Sahu, N. U., Singh, V., Ferraris, D. M., Rizzi, M., & Kharkar, P. S. (2018). Hit discovery of *Mycobacterium tuberculosis* inosine 5'-monophosphate dehydrogenase, GuaB2, inhibitors. *Bioorganic & Medicinal Chemistry Letters*, 28(10), 1714–1718.
- Saiakhov, R., Chakravarti, S., & Klopman, G. (2013). Effectiveness of CASE ultra expert system in evaluating adverse effects of drugs. *Molecular Informatics*, 32(1), 87–97.
- Saiakhov, R., Chakravarti, S., & Sedykh, A. (2014). An improved workflow to perform *in silico* mutagenicity assessment of impurities as per ICH M7 guideline. *Toxicology Letters*, 229(2014), S164.
- Serafini, M., Peluso, I., & Raguzzini, A. (2010). Flavonoids as anti-inflammatory agents. *Proceedings of the Nutrition Society*, 69(3), 273–278.
- Shah, C. S., & Kharkar, P. (2015). Inosine 5'-monophosphate dehydrogenase inhibitors as antimicrobial agents: Recent progress and future perspectives. *Future Medicinal Chemistry*, 7(11), 1415–1429.
- Shah, C. P., & Kharkar, P. S. (2018). Newer human inosine 5'-monophosphate dehydrogenase 2 (hIMPDH2) inhibitors as potential anticancer agents. *Journal of Enzyme Inhibition and Medicinal Chemistry*, 33(1), 972–977.
- Siddique, O., Ovalle, A., Siddique, A. S., & Moss, S. F. (2018). *Helicobacter pylori* infection: An update for the internist in the age of increasing global antibiotic resistance. *American Journal of Medicine*, 131(5), 473–479.
- Singh, M., Kaur, M., & Silakari, O. (2014). Flavones: An important scaffold for medicinal chemistry. *European Journal of Medicinal Chemistry*, 84, 206–239.
- Tharmalingam, N., Port, J., Castillo, D., & Mylonakis, E. (2018). Repurposing the anthelmintic drug niclosamide to combat *Helicobacter pylori*. *Scientific Reports*, 8(1), 1–12.
- Thung, I., Aramin, H., Vavinskaya, V., Gupta, S., Park, J. Y., Crowe, S. E., & Valasek, M. A. (2016). Review article: The global emergence of *Helicobacter pylori* antibiotic resistance. *Alimentary Pharmacology and Therapeutics*, 43(4), 514–533.
- Vakil, N., & Vaira, D. (2013). Treatment for *H. pylori* infection new challenges with antimicrobial resistance. *Journal of Clinical Gastroenterology*, 47(5), 383–388.
- Venkatachalam, H., Nayak, Y., & Jayashree, B. S. (2012). Synthesis, characterization and antioxidant activities of synthetic chalcones and flavones. *APCBEE Procedia*, 3, 209–213.
- Wroblewski, L. E., Peek, R. M., & Wilson, K. T. (2010). *Helicobacter pylori* and gastric cancer: Factors that modulate disease risk. *Clinical Microbiology Reviews*, 23(4), 713–739.
- Zagari, R. M., Rabitti, S., Eusebi, L. H., & Bazzoli, F. (2018). Treatment of *Helicobacter pylori* infection: A clinical practice update. *European Journal of Clinical Investigation*, 48(1), e12857.
- Zhang, R., Evans, G., Rotella, F. J., Westbrook, E. M., Beno, D., Huberman, E., ... Collart, F. R. (1999). Characteristics and crystal structure of bacterial inosine-5'-monophosphate dehydrogenase. *Biochemistry*, 38(15), 4691–4700.

SUPPORTING INFORMATION

Additional supporting information may be found online in the Supporting Information section at the end of the article.

How to cite this article: Sahu NU, Purushothaman G, Thiruvengatam V, Kharkar PS. Design, synthesis, and biological evaluation of *Helicobacter pylori* inosine 5'-monophosphate dehydrogenase (hIMPDH) inhibitors. *Drug Dev Res*. 2018; 1–8. <https://doi.org/10.1002/ddr.21467>